European Polymer Journal 129 (2020) 109636

Contents lists available at ScienceDirect

European Polymer Journal

journal homepage: www.elsevier.com/locate/europolj

Hydrophilic/hydrophobic modifications of a PnBA-b-PDMAEA copolymer and complexation behaviour with short DNA

Angeliki Chroni, Stergios Pispas*

Theoretical and Physical Chemistry Institute, National Hellenic Research Foundation, Athens, Greece

ARTICLE INFO

Keywords:
Amphiphilic block copolymers
Quaternization
Cationic polyelectrolytes
Gene delivery

ABSTRACT

We present studies on the quaternization of poly[(n-butyl acrylate)-*block*-(2-dimethylamino)ethyl acrylate], $PnBA_{40}$-b-$PDMAEA_{60}$ diblock (where subscripts denote %wt composition of the components), synthesized by reversible addition fragmentation chain transfer (RAFT) polymerization, the self-assembly of the quaternized copolymers, as well as their capability in binding with a short nucleic acid. Methyl iodide (CH_3I) and 1-iodohexane ($C_6H_{13}I$) are used for the quaternization of tertiary amines of the PDMAEA block. The quaternized $PnBA_{21}$-b-$Q_1PDMAEA_{79}$ and $PnBA_{33}$-b-$Q_6PDMAEA_{30}$ (where Q_1 and Q_6 prefixes denote the CH_3I and $C_6H_{13}I$ modifications) block polyelectrolytes are studied by fluorescence spectroscopy (FS) and their self-assembling behavior is investigated by dynamic and electrophoretic light scattering techniques (DLS and ELS). The $PnBA_{21}$-b-$Q_1PDMAEA_{79}$ polyelectrolytes seem to self-assemble into small spherical micelles with a PnBA core in aqueous media, whereas a less well defined aggregation behavior is observed for the $PnBA_{33}$-b-$Q_6PDMAEA_{30}$ copolymer, probably due to the presence of the six methylene hydrophobic side chains (C_6H_{13}) in the hydrophilic part of the copolymer, forming the micellar corona. The DNA binding capability of $PnBA_{21}$-b-$Q_1PDMAEA_{79}$ and $PnBA_{33}$-b-$Q_6PDMAEA_{30}$ chemically modified cationic block polyelectrolytes is studied and compared to the DNA complexation behaviour of the corresponding $PnBA_{40}$-b-$PDMAEA_{60}$ amino precursor. The formation and structure of polyplexes is studied by DLS, ELS, FS and UV–Vis techniques at various N/P ratios of positively-chargeable polymer amine (N = nitrogen) groups to negatively-charged nucleic acid phosphate (P) groups. The mass, size and surface potential of the polyplexes present a strong dependence on the N/P ratio. The stability of the polyplexes is determined by changes in their hydrodynamic parameters in the presence of salt. The $PnBA_{33}$-b-$Q_6PDMAEA_{30}$ quaternized copolymer exhibits a more effective binding with DNA, presumably due to the existence of both electrostatic interactions and reinforced hydrophobic interactions between $Q_6PDMAEA$ chains and DNA base pairs.

1. Introduction

Amphiphilic block copolymers (AmBCs) have come to the forefront of polymer science because of their interesting self-assembling ability into various nanostructures (such as micelles, vesicles, toroids, worms, polymeric nanoparticles, etc.) in an aqueous milieu [1]. Nowadays, self-assembled nanostructures of AmBCs are considered as alternative robust gene and drug carriers changing the fate of various therapies due to improved water solubility, extended duration in blood circulation, and biocompatibility characteristics [2,3]. Polymeric micelles remain at the focus point of polymer community, exhibiting significant advantages over other types of nanoparticles such as simple preparation, small size for deep tumor penetration, efficient drug and gene loading for effective therapeutic potency, high stability and controlled drug and gene release [4]. The hydrophobic segments of the polymeric micelles are segregated from the aqueous exterior to form an inner core surrounded by the hydrophilic entities (forming the shell). Hence, the hydrophobic core is stabilized by the hydrophilic shell, which serves as an interface between the bulk aqueous phase and the hydrophobic domain [5].

Hydrophilic moieties often include polyelectrolytes that develop substantial charge when dissolved or swollen in a highly polar solvent such as water. Amine-based cationic polymers such as polyethyleneimine (PEI), poly(L-lysine) (PLL), poly (dimethylaminoethyl methacrylate) (PDMAEMA), etc. are widely used to construct cationic micelles [6]. Quaternizing the tertiary amine groups of the copolymers

* Corresponding author at: Theoretical and Physical Chemistry Institute, National Hellenic Research Foundation, 48 Vassileos Constantinou Ave., 11635 Athens, Greece.
E-mail address: pispas@eie.gr (S. Pispas).

https://doi.org/10.1016/j.eurpolymj.2020.109636
Received 30 January 2020; Received in revised form 4 March 2020; Accepted 22 March 2020
Available online 23 March 2020
0014-3057/

hydrophilic segments creates a permanent positive charge on the polymer chain, which is crucial in designing cationic block polyelectrolytes based nanoparticles. Cationic blocks interact and complex with negatively charged nucleic acids forming polyplexes, while the charge-neutral hydrophilic blocks usually protect polyplexes from aggregation or precipitation allowing them to selectively target tissues [7].

Polycation nanoparticle delivery systems should ideally package the genetic material with the appropriate size for cellular internalization, provide specific targeting and stability, cell uptake, endolysosomal escape and ensure the release of the genetic material within the cell [8]. A successful gene transfer vehicle, however, depends on the physicochemical parameters of the cationic polymer/DNA complexes such as the ratio of positively-chargeable polymer amine (N = nitrogen) groups to negatively-charged nucleic acid phosphate (P) groups (N/P), size, stability, surface potential and salinity of the solution [7,9–12].

The advent of reversible addition fragmentation chain transfer polymerization (RAFT) facilitated the development of a wide range of synthetic polymers and polyelectrolytes with important application potential from materials to medicine. RAFT polymerization can be used with a variety of monomers, developing complex architectures through accurate control of the synthetic process and providing polymers with a well-controlled molecular weight and narrow molecular weight distributions [13].

In our previous work, a novel pH-responsive amphiphilic system with desirable properties emanating mainly from the PDMAEA block namely poly(n-butyl acrylate)-*block*-poly(2-dimethylaminoethyl acrylate) (PnBA-b-PDMAEA) copolymer, has been developed using the RAFT polymerization and it has been thoroughly characterized by various techniques [14]. In the current study, the $PnBA_{40}$-b-$PDMAEA_{60}$ diblock (where the subscripts denote %wt composition of the components) served as the basis for the subsequent modification reactions. Employing methyl iodide (CH_3I) and 1-iodohexane ($C_6H_{13}I$) as quaternization agents, the PDMAEA converts to a strong cationic polyelectrolyte, leading to $PnBA_{21}$-b-$Q_1PDMAEA_{79}$ and $PnBA_{33}$-b-$Q_6PDMAEA_{30}$ quaternized copolymers (where Q_1 and Q_6 prefixes denote the methyl iodide and 1-iodohexane quaternizing agents). The successful quaternization reactions and the chemical structure of the quaternized copolymers were confirmed by nuclear magnetic resonance spectroscopy (^{1}H NMR). The quaternized copolymers were studied by fluorescence spectroscopy (FS) and their self-assembling behaviour was examined by dynamic and electrophoretic light scattering techniques (DLS and ELS). The block copolymers synthesized form micelles in aqueous media with coronas having different hydrophilicity/hydrophobicity. The complexation of tertiary and quaternary amines of PDMAEA side groups with DNA molecules was studied by FS and ultraviolet (UV–Vis) spectroscopies before and after the quaternization procedures. Solution behaviour of the DNA/$PnBA_{40}$-b-$PDMAEA_{60}$, DNA/$PnBA_{21}$-b-$Q_1PDMAEA_{79}$ and DNA/$PnBA_{33}$-b-$Q_6PDMAEA_{30}$ polyplexes was also examined by DLS and ELS techniques under the influence of ionic strength.

2. Experimental section

2.1. Materials

Methyl iodide (CH_3I) and iodohexane ($C_6H_{13}I$) were used as the quaternizing agents obtained from Aldrich. Pyrene was used as the hydrophilic fluorescent probe and ethidium bromide (EtBr) as the fluorescent DNA intercalating dye for complexation assays, both received from Sigma-Aldrich. Deoxyribonucleic acid sodium salt (DNA, with ~113 bp) from salmon testes, was received from Sigma-Aldrich.

2.2. Self-assembly of the amphiphilic diblock copolymers

The self-assembly of the amphiphilic $PnBA_{40}$-b-$PDMAEA_{60}$ diblock copolymer is reported in our previous work [14]. The quaternized $PnBA_{21}$-b-$Q_1PDMAEA_{79}$ and $PnBA_{33}$-b-$Q_6PDMAEA_{30}$ polyelectrolyte diblocks were self-assembled by directly dissolving the dry polymer in distilled H_2O at 10^{-3} g/ml concentration. All copolymer solutions were studied after allowing them to stand overnight for equilibration.

2.3. Characterization methods

^{1}H NMR spectra were carried out on a Varian 300 (300 mHz) spectrometer operated by Vjnmr software, using tetramethylsilane (TMS) as the internal standard and deuterated chloroform ($CDCl_3$) and acetone as the solvents. The composition of $PnBA_{40}$-b-$PDMAEA_{60}$ diblock copolymer was reported in a previous work [14].

The composition of $PnBA_{21}$-b-$Q_1PDMAEA_{79}$ BCs was calculated using the characteristic spectral peaks at 0.9 ppm which corresponds to the $-CH_3$ protons of PnBA side chain (3H, $-CH_3-$) and at 2.84 ppm which corresponds to the $-(CH_3)_3$ protons of Q_1PDMAEA group (9H, $-CH_3-CH_3-CH_3$).

^{1}H NMR spectra peaks of $PnBA_{21}$-b-$Q_1PDMAEA_{79}$: (Acetone, ppm): 4.06 (2H, $-CH_2-$, 2H,$-CH_2-$) PnBA and PDMAEA main chain (a), 1.63 (2H, $-CH_2-$) PnBA side chain (b), 1.4 (2H, $-CH_2-$) PnBA side group (c), 0.9 (3H, $-CH_3-$) PnBA side chain (d), 3.45 (2H, $-CH_2-$) PDMAEA side chain (e), 2.84 (9H, $-CH_3-CH_3-CH_3-$) PDMAEA side chain (f).

The composition of $PnBA_{33}$-b-$Q_6PDMAEA_{30}$ BCs was calculated using the characteristic spectral peaks at 0.96 ppm which corresponds to the $-CH_3$ protons of PnBA side chain (3H, $-CH_3-$), at 2.4 ppm that corresponds to the $-(CH_3)_2$ protons of PDMAEA amino group (6H, $-CH_3-CH_3$) and at 3.5 ppm that corresponds to the $-(CH_3)_2$ protons of Q_6PDMAEA amino group (6H, $-CH_3-CH_3$).

^{1}H NMR spectra peaks of $PnBA_{33}$-b-$Q_6PDMAEA_{30}$: (Acetone, ppm): 4.0 (2H,$-CH_2-$) PDMAEA side chain (e), 3.7 (2H, $-CH_2-$) Q_6PDMAEA side chain (i), 3.5 (6H, $-CH_3-CH_3-$) Q_6PDMAEA side chain (j), 3.38 (13H, $-CH_2-CH_2-CH_2-CH_2-CH_2-CH_3$) Q_6PDMAEA side chain (k), 3.2 (2H, $-CH_2-$) PDMAEA side chain (f), 2.4 (6H, $-CH_3-CH_3-$) PDMAEA side chain (g), 2.3–1.6 (1H, $-CH-$, 2H, $-CH_2-$) PnBA and PDMAEA main chain (d) and (h), 1.6 (2H, $-CH_2-$) PnBA side chain (a), 1.4 (2H, $-CH_2-$) PnBA side chain (b), 0.96 (3H, $-CH_3-$) PnBA side chain (c).

DLS measurements in the angular range 45–135° were conducted on an ALV/CGS-3 Compact Goniometer System (ALV GmbH, Germany), using a JDS Uniphase 22 mW He-Ne laser as light source, operating at 632.8 nm, equipped with an ALV-5000/EPP multi-tau digital correlator with 288 channels and an ALV/LSE-5003 light scattering electronics unit for stepper motor drive and limit switch control. Measurements were carried out five times for each concentration/angle and were averaged. Before any measurements, the solutions were filtered through 0.45 mm hydrophilic PTFE Millex syringe filters to remove dust particles or large aggregates and they were equilibrated for 15 min. Toluene was used as the calibration standard solvent. The size data and figures shown below are from measurements at 90°. Obtained correlation functions were analyzed by the cumulants method and CONTIN software. Ionic strength effects on quaternized copolymers and on polyplexes were studied by adding a stock NaCl 1 M solution in the quaternized copolymer solution in aliquots and thus increasing salt concentration (in the range 0.01–0.5 M NaCl) in the aqueous copolymer solutions.

ELS measurements were made using a Nano Zeta Sizer (Malvern Instruments Ltd., Malvern, UK) at 633 nm and a fixed backscattering angle of 173°. Zeta-potential values that recorded are the average of 50 runs, using the Henry correction of Smoluchowski equation after equilibration at 25 °C.

FS experiments were performed in order to determine the critical micelle concentrations (CMC) of the block copolymers in water before and after the quaternization procedures using a Fluorolog-3 Jobin Yvon-Spex spectrofluorometer (modelGL3–21). The excitation wavelength used for these measurements was 335 nm and emission spectra were recorded in the region 355–630 nm. Pyrene was used as the

fluorescent probe. A stock solution of 1 mM pyrene in acetone was prepared and was added in the solutions in a ratio of 1 μl per 1 ml polymer solution. Measurements were conducted after evaporation of acetone overnight at room temperature.

The complexation behaviour of the copolymers with DNA molecules at various N/P ratios has been studied using the fluorescence of ethidium bromide. An initial stock solution of DNA (1×10^{-4} g/ml) was prepared followed by addition of EtBr ([EtBr] = [P]/4). Subsequently, the DNA aqueous solution was titrated using a concentrated polymer solution, up to an N/P ratio equal to 8. The titration was followed by fluorescence spectroscopy. The excitation wavelength used for the solutions of polyplexes was at 535 nm, monitoring the emission at 600 nm.

UV–Vis absorption spectra of polyplexes were recorded between 200 and 400 nm wavelength using a Perkin Elmer (Lambda 19) UV–Vis–NIR spectrophotometer (Waltham, MA, USA). The polyplexes were measured at N/P ratios in the 0.25–4 range and were diluted to get an absorbance value of less than 1.

2.4. Quaternizations of PnBA40-b-PDMAEA60 diblock copolymer

Appropriate stoichiometric calculations were made such that the $PnBA_{21}$-b-$Q_1PDMAEA_{79}$ and $PnBA_{33}$-b-$Q_6PDMAEA_{30}$ copolymers quaternizes at 100% degree using CH_3I and at 25% degree using $C_6H_{13}I$. In a typical quaternization procedure, the block copolymer is dissolved in THF (2% w/v) and the quaternizing agent is added to the solution (CH_3I moles/PDMAEA moles = 2 in case of the $PnBA_{21}$-b-$Q_1PDMAEA_{79}$ and $C_6H_{13}I$ moles/PDMAEA moles = 0.3 in the case of $PnBA_{33}$-b-$Q_6PDMAEA_{30}$) [15,16]. The reactions, as illustrated in Scheme 1, took place for 24 h at room temperature, under stirring. After that period, a rotary evaporator was used for the evaporation of THF and the products were dried in a vacuum oven for another 24 h.

2.5. Polyplex formation

The nucleic acids/polymer polyplexes were formed by mixing gently the copolymer and DNA stock solutions in the desired N/P ratios [17]. The polyplexes were prepared at N/P ratios in the 0.25–4 range by maintaining the polymer concentration stable at ambient temperature under stirring. The copolymer stock solutions at pH 7 were prepared as follows: 4 mg of the $PnBA_{40}$-b-$PDMAEA_{60}$ polymer was directly dissolved in 8 ml NaCl ($C = 5 \times 10^{-4}$ g/ml) and 8 mg of the quaternized copolymers ($PnBA_{21}$-b-$Q_1PDMAEA_{79}$ and $PnBA_{33}$-b-$Q_6PDMAEA_{30}$) were directly dissolved in 8 ml NaCl ($C = 10^{-3}$ g/ml). The DNA stock solution was prepared at 2×10^{-4} g/ml for the mixing and formation of DNA/$PnBA_{40}$-b-$PDMAEA_{60}$, DNA/$PnBA_{21}$-b-$Q_1PDMAEA_{79}$ and DNA/$PnBA_{33}$-b-$Q_6PDMAEA_{30}$ polyplexes. Indicatively, 1 ml of the copolymer stock solution was added to each N/P ratio before mixing with the appropriate volume of DNA solution. Scheme 2 is a graphical illustration of DNA binding with cationic copolymers to form polyplexes.

The $PnBA_{40}$-b-$PDMAEA_{60}$ copolymer stock solution of NaCl 0.01 M was studied at 5×10^{-4} g/ml concentration whereas the quaternized $PnBA_{21}$-b-$Q_1PDMAEA_{79}$ and $PnBA_{33}$-b-$Q_6PDMAEA_{30}$ copolymer stock solutions of NaCl 0.01 M were studied at 10^{-3} g/ml. The DNA/$PnBA_{40}$-b-$PDMAEA_{60}$, DNA/$PnBA_{21}$-b-$Q_1PDMAEA_{79}$ and DNA/$PnBA_{33}$-b-$Q_6PDMAEA_{30}$ polyplexes were studied in the 0.25–4 N/P ratios. The self-assembly of the polyplexes was studied after allowing them to stand overnight for equilibration.

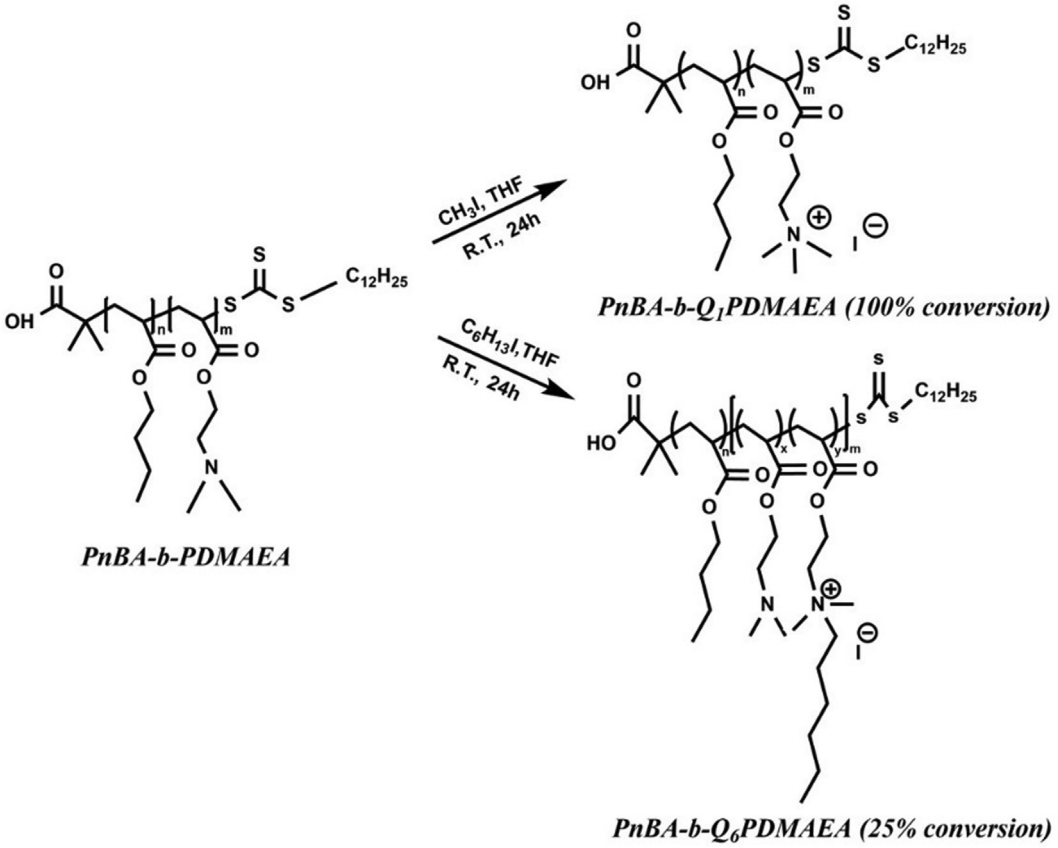

Scheme 1. Schematic illustration of the quaternization reactions using CH_3I and $C_6H_{13}I$ to form $PnBA_{21}$-b-$Q_1PDMAEA_{79}$ and $PnBA_{33}$-b-$Q_6PDMAEA_{30}$ cationic copolymers respectively.

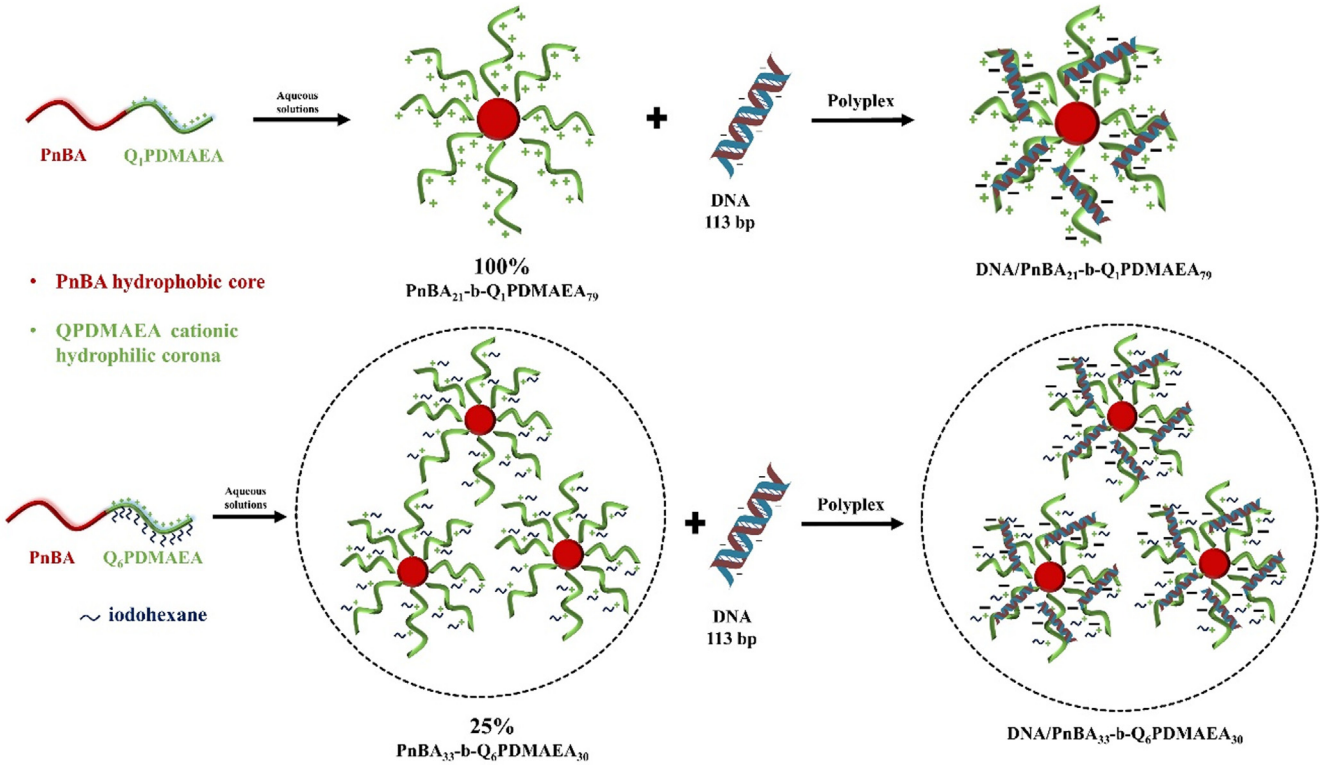

Scheme 2. Schematic illustration of polyplex formation.

3. Results and discussion

3.1. Synthesis of $PnBA_{40}$-b-$PDMAEA_{60}$ diblock copolymer

The synthesis of the $PnBA_{40}$-b-$PDMAEA_{60}$ diblock, using the RAFT polymerization technique, as well as its molecular and physicochemical characterization are presented and discussed in our previous work [14].

3.2. Quaternization reactions and molecular characterization

The PDMAEA block was quaternized to quaternary ammonium after a period of 24 h and converted to a strong cationic polyelectrolyte salt using both CH_3I and $C_6H_{13}I$ quaternizing agents. In Scheme 1, a graphical representation of the quaternization reaction and the formation of $PnBA_{21}$-b-$Q_1PDMAEA_{79}$ and $PnBA_{33}$-b-$Q_6PDMAEA_{30}$ polyelectrolytes is depicted.

^1H NMR spectroscopy confirmed the successful quaternization of the amino side group of PDMAEA block using CH_3I and $C_6H_{13}I$. The molecular weights and the compositions of the quaternized copolymers were calculated using the obtained molecular characteristics of the $PnBA_{40}$-b-$PDMAEA_{60}$ diblock copolymer as determined by SEC and ^1H NMR measurements [14]. In the case of $PnBA_{21}$-b-$Q_1PDMAEA_{79}$ copolymers, the M_w and the composition were calculated taking into consideration that the reaction is essentially quantitative. In the case of $PnBA_{33}$-b-$Q_6PDMAEA_{30}$ copolymers, the M_w and the composition were calculated in accordance to the degree of quaternization from NMR, i.e. 25%. The molecular weights and composition of the copolymers, as well as the number of the quaternized monomeric units are summarized

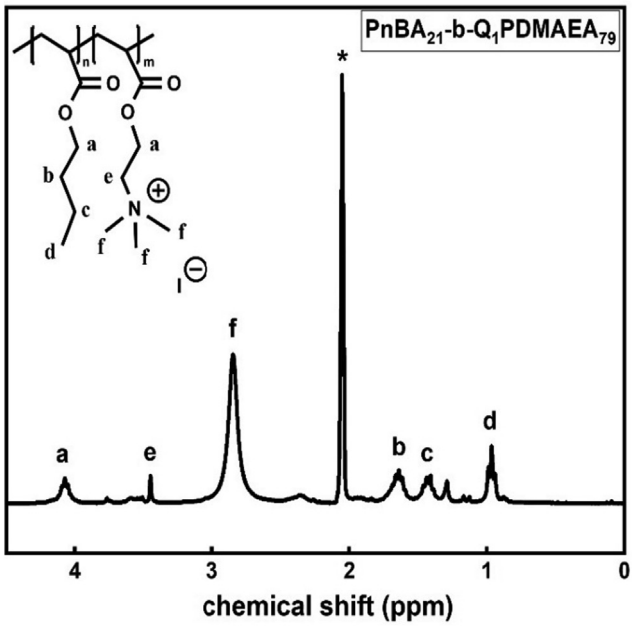

Fig. 1. ^1H-NMR spectrum of the $PnBA_{21}$-b-$Q_1PDMAEA_{79}$ copolymer in acetone-d_6.

Table 1
Molecular characteristics of the $PnBA_{21}$-b-$Q_1PDMAEA_{79}$ and $PnBA_{33}$-b-$Q_6PDMAEA_{30}$ copolymers.

Sample	M_w pol (g/mol)	M_W PDMAEA (g/mol)	M_W QPDMAEA (g/mol)	% wt PnBA	% wt PDMAEA	% wt QPDMAEA	Quaternized monomeric units
$PnBA_{21}$-b-$Q_1PDMAEA_{79}$	12,500	–	9400	21	–	79	33
$PnBA_{33}$-b-$Q_6PDMAEA_{30}$	9500	3500	2800	33	37	30	8

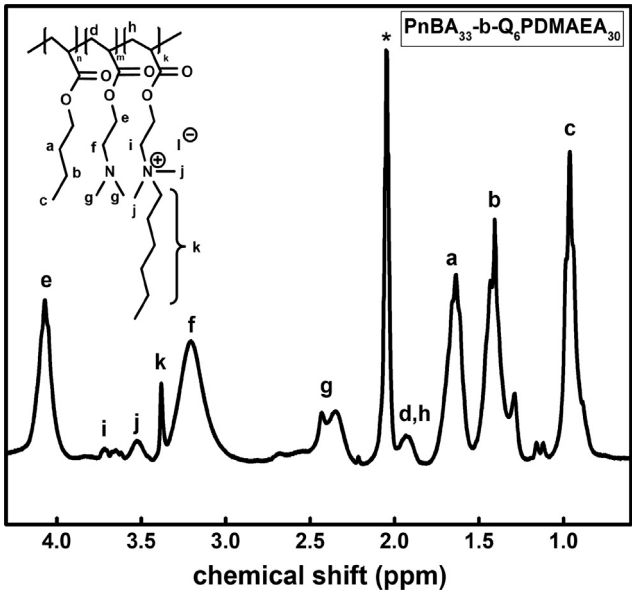

Fig. 2. ^{1}H-NMR spectrum of the $PnBA_{33}$-b-$Q_6PDMAEA_{30}$ copolymer in acetone-d_6.

in Table 1. Representative ^{1}H NMR spectra of the quaternized $PnBA_{21}$-b-$Q_1PDMAEA_{79}$ and $PnBA_{33}$-b-$Q_6PDMAEA_{30}$ copolymers are presented in Figs. 1 and 2 respectively.

3.3. Self-assembly of the quaternized copolymers

FS, DLS and ELS measurements were performed to assess the CMC, the size, the shape and the surface charge of the diblock copolymer aggregates formed in aqueous media. To examine the versatile properties of the quaternized copolymers, CMC was determined as the inflection point in the I_1/I_3 vs concentration curves using the FS technique and pyrene was used as the fluorescent probe. The polymer stock solutions concentrations were at 10^{-3} g/ml and at pH = 7. Calculated relative intensity ratio I_1/I_3 of pyrene peaks versus the copolymer concentration in water for the $PnBA_{40}$-b-$PDMAEA_{60}$, $PnBA_{21}$-b-$Q_1PDMAEA_{79}$, $PnBA_{33}$-b-$Q_6PDMAEA_{30}$ copolymers is shown in Fig. 3. All CMC values are gathered in Table 2. The CMC of the $PnBA_{21}$-b-$Q_1PDMAEA_{79}$ copolymer has been increased compared to the CMC value of the $PnBA_{40}$-b-$PDMAEA_{60}$ diblock precursor as the charged side

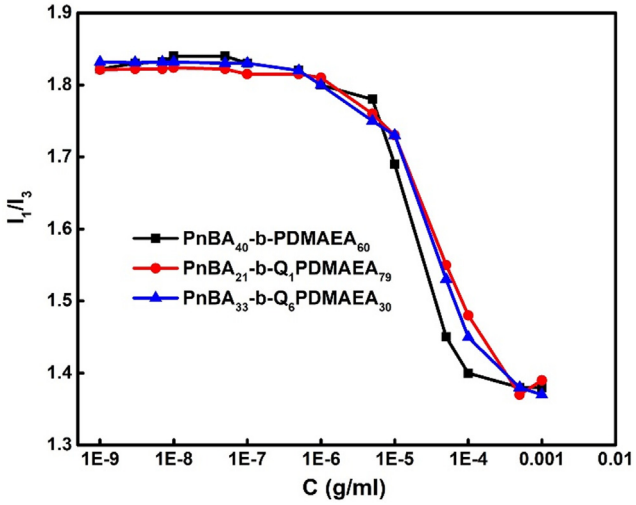

Fig. 3. CMC determination for the $PnBA_{40}$-b-$PDMAEA_{60}$, $PnBA_{21}$-b-$Q_1PDMAEA_{79}$, and $PnBA_{33}$-b-$Q_6PDMAEA_{30}$ copolymers.

Table 2
FS, DLS and ELS results of $PnBA_{40}$-b-$PDMAEA_{60}$, $PnBA_{21}$-b-$Q_1PDMAEA_{79}$ and $PnBA_{33}$-b-$Q_6PDMAEA_{30}$ copolymers.

Sample	CMC ($\times 10^{-6}$ g/ml) (FS)	R_h (nm) (DLS)	PDI (DLS)	ζ_{pot} (mV) (ELS)
$PnBA_{40}$-b-$PDMAEA_{60}$	5.3	93	0.321	+18
$PnBA_{21}$-b-$Q_1PDMAEA_{79}$	7.8	21	0.241	+43
$PnBA_{33}$-b-$Q_6PDMAEA_{30}$	6.0	93	0.371	+10

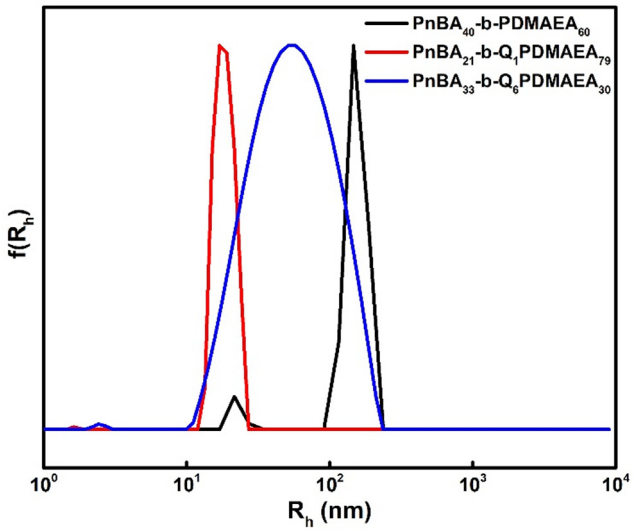

Fig. 4. A comparison of the size distributions from CONTIN analysis for $PnBA_{40}$-b-$PDMAEA_{60}$, $PnBA_{21}$-b-$Q_1PDMAEA_{79}$ and $PnBA_{33}$-b-$Q_6PDMAEA_{30}$ copolymers 90° in aqueous solutions.

chains enhance copolymer solubility. Conversely, the CMC of the $PnBA_{33}$-b-$Q_6PDMAEA_{30}$ copolymer has been reduced compared to the CMC value of the $PnBA_{21}$-b-$Q_1PDMAEA_{79}$ quaternized copolymer due to the presence of the six carbons hydrophobic functional side chains added to the PDMAEA blocks that reduce the polymer solubility and render the system more hydrophobic.

The hydrodynamic radius (R_h) and size polydispersity index (PDI) values of the formed nanostructures in aqueous media are presented in Table 2. A comparison of the size distributions of the $PnBA_{40}$-b-$PDMAEA_{60}$, $PnBA_{21}$-b-$Q_1PDMAEA_{79}$ and $PnBA_{33}$-b-$Q_6PDMAEA_{30}$ quaternized copolymers in aqueous solutions is presented in Fig. 4 at 90°. DLS data revealed almost monomodal distributions for all quaternized copolymer solutions which indicate the participation of all chains in the formation of micellar nanostructures. According to our previous work, the $PnBA_{40}$-b-$PDMAEA_{60}$ diblock copolymer presented remarkable morphological transitions in aqueous solutions of varying pH values. Particularly, at neutral pH, spherical nanoparticles, multicomponent vesicles and larger vesicles appeared as proved by Cryo-TEM experiments, whereas mainly nanostructures of 93 nm appeared according to DLS data in Table 2 [14]. The $PnBA_{21}$-b-$Q_1PDMAEA_{79}$ and $PnBA_{33}$-b-$Q_6PDMAEA_{30}$ copolymers exhibited lower R_h and intensity values compared to the $PnBA_{40}$-b-$PDMAEA_{60}$ diblock due to the enhanced hydrophilicity after the quaternization reactions, at least in the case of $PnBA_{21}$-b-$Q_1PDMAEA_{79}$. The $PnBA_{21}$-b-$Q_1PDMAEA_{79}$ polyelectrolytes seem to self-assemble into micelles of R_h = 20 nm in aqueous media whereas a relatively larger mean size and broader size distribution is observed for the $PnBA_{33}$-b-$Q_6PDMAEA_{30}$ copolymer, presumably due to the presence of the hydrophobic C_6H_{13} side chains in the PDMAEA block of the copolymer, which is a distinctive difference compared to the case of the $PnBA_{21}$-b-$Q_1PDMAEA_{79}$ copolymer. Apparently, hydrophobic interactions between the coronas lead to a secondary

aggregation and to less well-defined structures in terms of size distribution. All ζ_{pot} values (Table 2) are positive as the dimethylamino groups of $PnBA_{40}$-b-$PDMAEA_{60}$ copolymer are partially protonated and fully or more protonated/charged in the case of $PnBA_{21}$-b-$Q_1PDMAEA_{79}$ and $PnBA_{33}$-b-$Q_6PDMAEA_{30}$ copolymers, respectively. Particularly, the zeta potential value of the $PnBA_{33}$-b-$Q_6PDMAEA_{30}$ copolymer appears less positive than the $PnBA_{40}$-b-$PDMAEA_{60}$ diblock, probably due to the presence of the six-methylene hydrophobic functional side chains ($C_6H_{13}I$) in the hydrophilic part of the chemically converted copolymer, after the quaternization reaction. These hydrophobic segments may cover some positive charges on the $Q_6PDMAEA$ chains, turning the surface potential less positive than that of the $PnBA_{40}$-b-$PDMAEA_{60}$ diblock which has not undergone any chemical modification.

3.4. Effect of solution ionic strength on the nanostructures of the copolymers

The addition of NaCl in aqueous polyelectrolyte copolymer solutions often elicits significant changes in polymer solubility and size of the polymeric chains [18,19]. The effect of ionic strength on $PnBA_{40}$-b-$PDMAEA_{60}$ copolymer and its derivatives, $PnBA_{21}$-b-$Q_1PDMAEA_{79}$ / $PnBA_{33}$-b-$Q_6PDMAEA_{30}$, was studied by DLS experiments, as higher NaCl concentration was gradually introduced in the aqueous solutions of the copolymers synthesized. The measurements of the $PnBA_{40}$-b-$PDMAEA_{60}$ copolymer were conducted at a solution concentration of 5×10^{-4} g/ml whereas the quaternized $PnBA_{21}$-b-$Q_1PDMAEA_{79}$ /$PnBA_{33}$-b-$Q_6PDMAEA_{30}$ copolymers were prepared at 10^{-3} g/ml. All measurements were carried out at 90°, pH = 7 and 25 °C. In Fig. 5, the dependence of R_h and scattered intensity on the NaCl concentration is depicted for the $PnBA_{40}$-b-$PDMAEA_{60}$, $PnBA_{21}$-b-$Q_1PDMAEA_{79}$ and $PnBA_{33}$-b-$Q_6PDMAEA_{30}$ copolymers. The effect of ionic strength on the $PnBA_{40}$-b-$PDMAEA_{60}$ diblock is rooted in the weak polyelectrolyte nature of the PDMAEA block. Specifically, a secondary aggregation is observed in Fig. 5a, as salt concentration increases, indicating a significant growth in diameters and mass, until both R_h and intensity values reach a plateau. Regarding Fig. 5b, quaternized $PnBA_{21}$-b-$Q_1PDMAEA_{79}$ copolymer shows no evidence of shrinkage and quite stable values of R_h are presented by the copolymer nanostructures in solution. Particularly, the gradual addition of salt does modulate significantly repulsive electrostatic interactions between the hydrophilic chains, and $Q_1PDMAEA$ block tethering to PnBA hydrophobic cores does not allow shrinkage of the hydrophilic corona chains.

On the other hand, an increase in the mass of the $PnBA_{33}$-b-$Q_6PDMAEA_{30}$ copolymer nanostructures is observed in Fig. 5c, as the scattered intensity gradually increases significantly with the addition of salt. The quaternized copolymer aggregates in this case exhibit shrink-resistance and show relatively stable R_h values as the ionic strength increases, possibly due to shrinkage of the partially hydrophobized coronas which compensates the mass increase. The observed behavior is a delicate balance between charge screening from NaCl addition, hydrophobic interactions due to the hydrophobic side chains of the corona blocks and increased hydrophilicity coming from the permanent positive charges introduced after the quaternization with $C_6H_{13}I$.

3.5. Complexation with DNA – Ethidium bromide quenching assay

Ethidium bromide (EtBr) is a fluorescent compound interacting with DNA by intercalation between the base pairs rendering the dye strongly fluorescent. Upon complexation with cations, the fluorescence intensity decreases due to inhibition of its binding with DNA. As a result, quenching of EtBr fluorescence is usually used to monitor the formation of polyplexes [17,20]. Fig. 6 represents typical curves of the relative fluorescence intensity as a function of the N/P ratio along with the corresponding spectra of DNA/$PnBA_{40}$-b-$PDMAEA_{60}$, DNA/$PnBA_{21}$-b-$Q_1PDMAEA_{79}$ and DNA/$PnBA_{33}$-b-$Q_6PDMAEA_{30}$ polyplexes. Most of the curves exhibit a well-pronounced decrease of the fluorescent intensity that is steeper for the case of DNA/$PnBA_{33}$-b-$Q_6PDMAEA_{30}$ polyplexes. In Fig. 6a, the DNA/$PnBA_{40}$-b-$PDMAEA_{60}$ polyplexes are associated with an extremely slow decay of the fluorescent intensity in comparison with the quaternized polyplexes, possibly due to the low complexation efficiency of the partially positively charged amino groups with DNA molecules. Instead, $PnBA_{21}$-b-$Q_1PDMAEA_{79}$ copolymer exhibits a stronger complexation with DNA (Fig. 6b) and a faster rate of EtBr molecules displacement than the DNA/$PnBA_{40}$-b-$PDMAEA_{60}$ polyplexes. The steeper decrease in fluorescence intensity indicates a strong DNA binding with the positively charged amino groups of the quaternized copolymer. Undoubtedly, Fig. 6c displays the strongest DNA complexation with the positive charged and partially hydrophobized amino groups of the quaternized $PnBA_{33}$-b-$Q_6PDMAEA_{30}$ copolymer than the previously studied polyplexes. The faster decay rate of the fluorescence intensity (Fig. 6c) indicates the ability of the $PnBA_{33}$-b-$Q_6PDMAEA_{30}$ copolymer to strongly bind with DNA molecules, depicting also a potential effect of hydrophobic interactions being active in this case. The critical quenching of the fluorescence is associated with the displacement of intercalated EtBr from the double helix indicating a strong complexation ability of the investigated copolymers.

3.6. UV absorption spectra

DNA complexation with cationic polyelectrolytes is often examined by UV–Vis spectroscopy as it studies the absorption of nucleic acids providing information about the type of interaction between the DNA and the copolymers and indicates possible changes in the configuration of DNA chains.

According to the literature, free DNA exhibits a characteristic absorption peak at λ_{max} = 260 nm [21,22], whose intensity decreases while it forms polyplexes with the positive charged polymer chains and

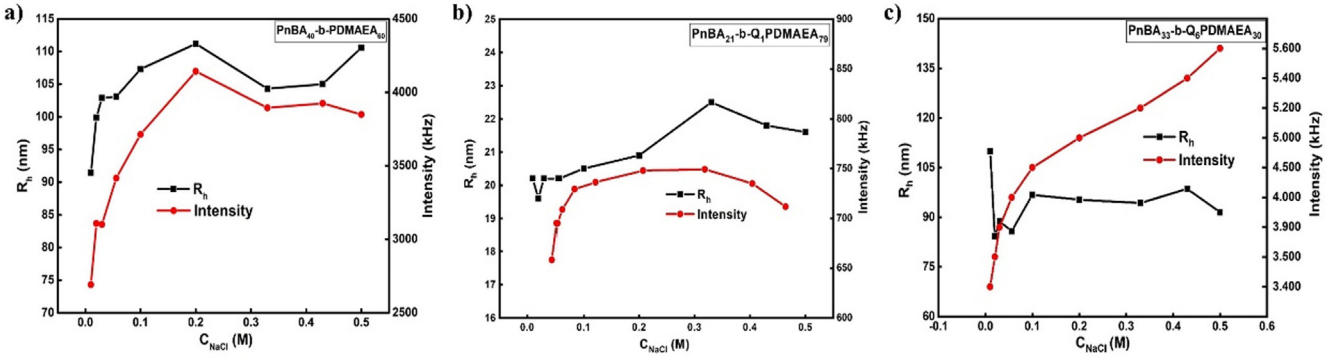

Fig. 5. R_h and scattered intensity as a function of ionic strength ([NaCl]) for (a) $PnBA_{40}$-b-$PDMAEA_{60}$, (b) $PnBA_{21}$-b-$Q_1PDMAEA_{79}$ and (c) $PnBA_{33}$-b-$Q_6PDMAEA_{30}$ copolymers in aqueous solutions.

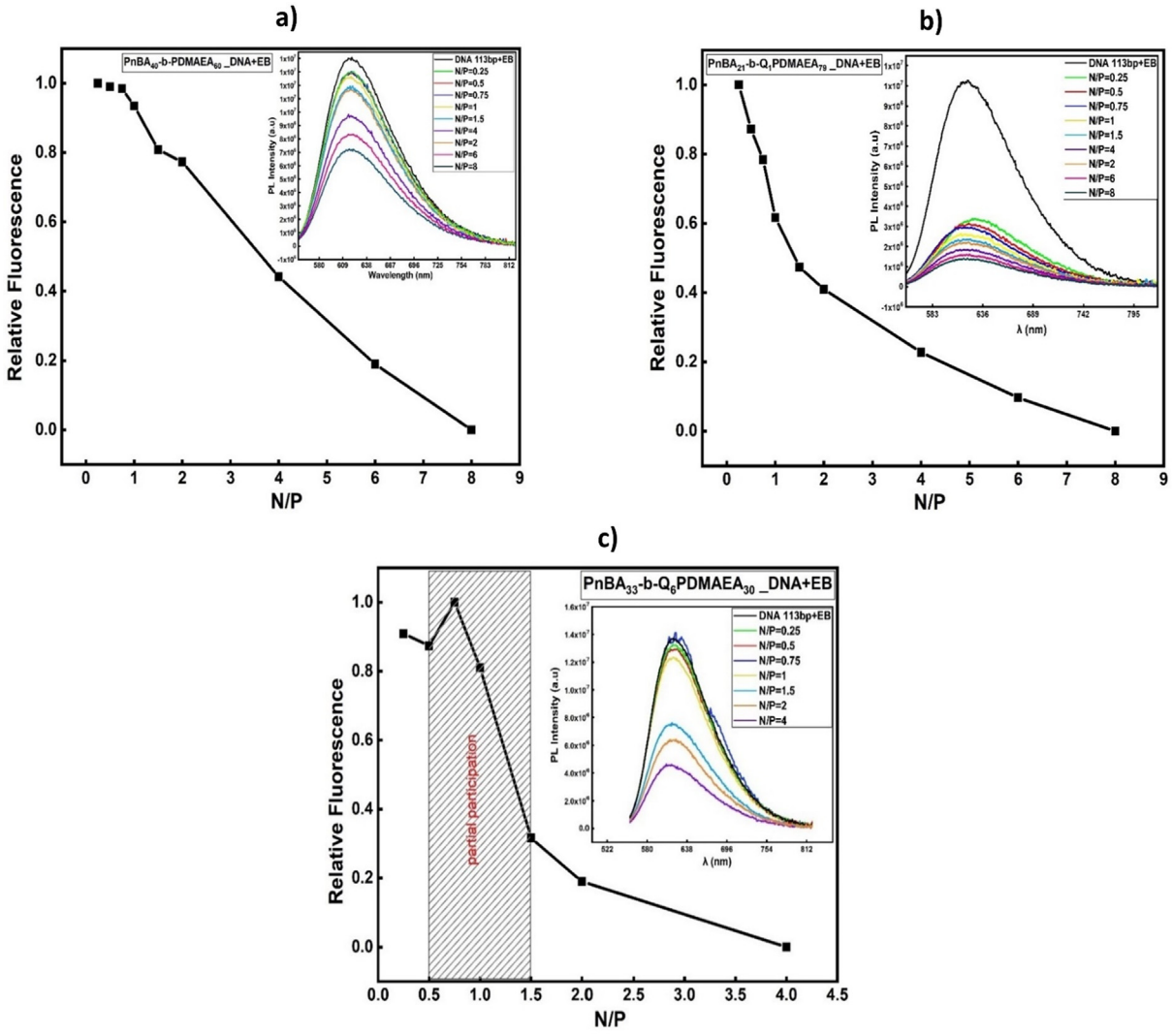

Fig. 6. Ethidium bromide fluorescence quenching in (a) DNA/$PnBA_{40}$-b-$PDMAEA_{60}$, (b) DNA/$PnBA_{21}$-b-$Q_1PDMAEA_{79}$ and (c) $PnBA_{33}$-b-$Q_6PDMAEA_{30}$ polyplexes.

a new peak appears at shorter wavelengths. Fig. 7a presents the UV absorption spectra of the DNA/$PnBA_{40}$-b-$PDMAEA_{60}$ polyplexes at N/P ratios ranging from 0.25 to 4, where no appreciable interaction with the negative DNA phosphate groups is observed with the partially charged PDMAEA block. However, the presence of two UV absorption peaks in Fig. 7b indicates the existence of both free and complexed DNA in the presence of $PnBA_{21}$-b-$Q_1PDMAEA_{79}$ quaternized copolymer. The formation of polyplexes is observed at all N/P ratios whereas free DNA prevails at 0.25 ratio due to the presence of a large excess of DNA phosphate groups. The presence of one UV absorption peak at N/P ratio equal to 1 suggests that no free DNA remained in the solution resulting in DNA/$PnBA_{21}$-b-$Q_1PDMAEA_{79}$ polyplexes. To the best of our knowledge, there is insufficient information in the literature about the interpretation of the UV peak at ca. 230 nm. We believe that this newly developed peak is probably related to the configuration transitions of DNA when it is complexed with the cationic polymers, since the

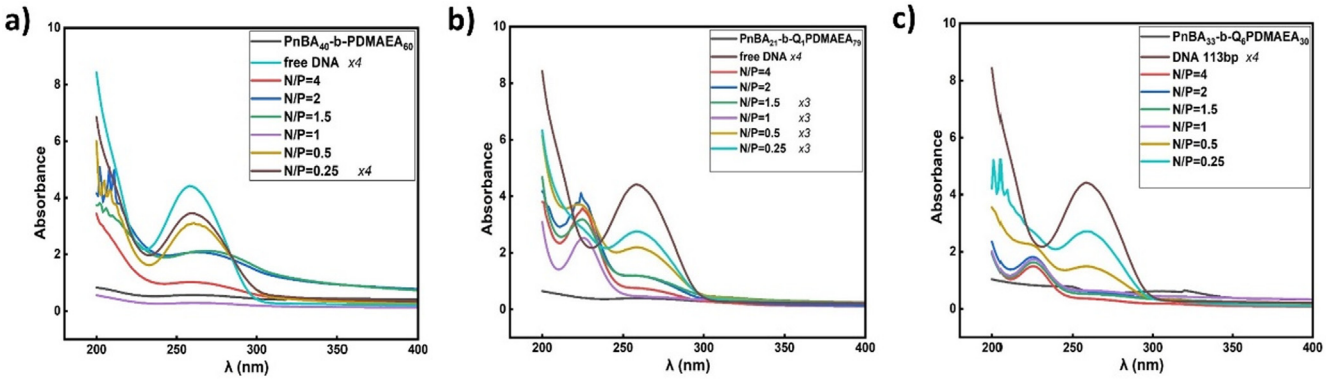

Fig. 7. UV spectra of (a) DNA/$PnBA_{40}$-b-$PDMAEA_{60}$, DNA/$PnBA_{21}$-b-$Q_1PDMAEA_{79}$ and $PnBA_{33}$-b-$Q_6PDMAEA_{30}$ polyplexes at N/P ratios in the 0.25–4 range.

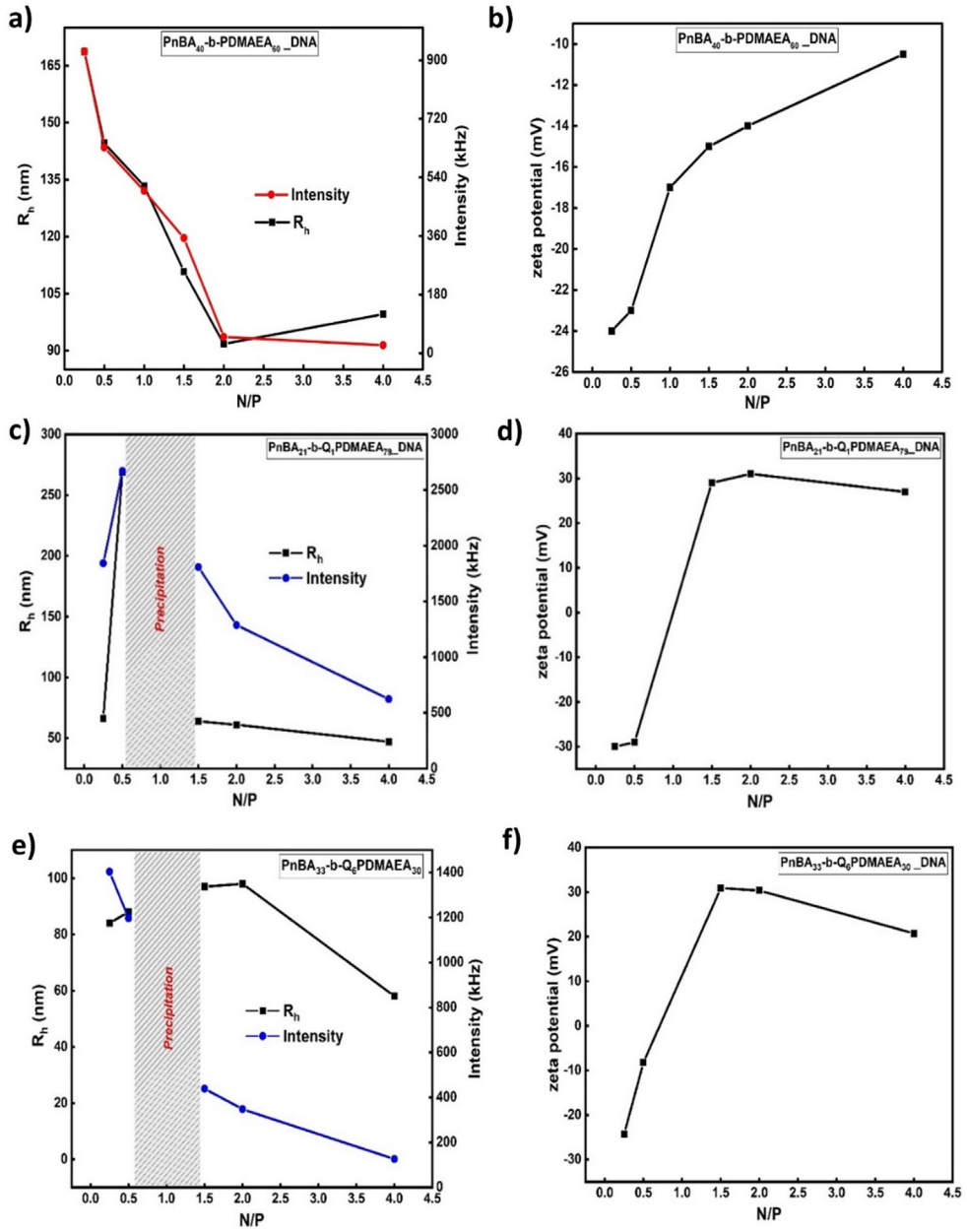

Fig. 8. Variations of the R_h and scattered intensity (a, c, e) and ζ potential (b), (d), (f) with the N/P ratio of the DNA/$PnBA_{40}$-b-$PDMAEA_{60}$, DNA/$PnBA_{21}$-b-$Q_1PDMAEA_{79}$ and DNA/$PnBA_{33}$-b-$Q_6PDMAEA_{30}$ polyplexes.

amphiphilic block copolymers do not show any peaks in this particular spectral range. A strong complexation of DNA with the positively charged amino groups of $PnBA_{33}$-b-$Q_6PDMAEA_{30}$ copolymer is observed in Fig. 7c at all N/P ratios except for 0.5 ratio where both free and complexed DNA existed and of 0.25 ratio where free DNA prevails in the solution.

3.7. Size and ζ-potential of polyplexes

The complexation of the quaternized copolymers with nucleic acids is achieved through electrostatic coupling of the positively charged amino groups of the copolymer and the negatively charged phosphate groups of DNA. The ability of PDMAEA-based block copolymers and their derivatives to condense DNA molecules and act as potential gene delivery vectors was examined by DLS and ELS techniques. The polyplexes (DNA/$PnBA_{40}$-b-$PDMAEA_{60}$, DNA/$PnBA_{21}$-b-$Q_1PDMAEA_{79}$ and DNA/$PnBA_{33}$-b-$Q_6PDMAEA_{30}$) were prepared at N/P ratios in the 0.25–4 range with DNA of low molar mass (≈113 bp). The complexation of the partially positively charged $PnBA_{40}$-b-$PDMAEA_{60}$ diblock with nucleic acids was examined and then compared to DNA/$PnBA_{21}$-b-$Q_1PDMAEA_{79}$ and DNA/$PnBA_{33}$-b-$Q_6PDMAEA_{30}$ polyplexes. The DLS and ELS results for the DNA/$PnBA_{40}$-b-$PDMAEA_{60}$, DNA/$PnBA_{21}$-b-$Q_1PDMAEA_{79}$ and DNA/$PnBA_{33}$-b-$Q_6PDMAEA_{30}$ polyplexes are displayed in Fig. 8. As DLS data reveal for the DNA/$PnBA_{40}$-b-$PDMAEA_{60}$ and DNA/$PnBA_{21}$-b-$Q_1PDMAEA_{79}$ polyplexes (Fig. 8a and 8c), the intensity and hydrodynamic radius (R_h) decrease as the N/P ratio increases. Specifically, the formation of lower mass and smaller size complexes is observed when gradually adding $PnBA_{40}$-b-$PDMAEA_{60}$ and quaternized $PnBA_{21}$-b-$Q_1PDMAEA_{79}$ copolymers respectevily. The R_h of DNA/$PnBA_{33}$-b-$Q_6PDMAEA_{30}$ polyplexes slightly increases as the N/P ratio rises from 0.25 to 2 and then it decreases until N/P ratio 4. On the other hand, the intensity steeply declines until N/P ratio 2 followed by a lower-rate of decrease until N/P ratio 4. The formation of lower mass and larger complexes is detected as the ratio of

copolymer increases to N/P ratio 2. Notably, precipitation was observed around the neutralization point (N/P = 1) for the DNA/$PnBA_{21}$-b-$Q_1PDMAEA_{79}$ and DNA/$PnBA_{33}$-b-$Q_6PDMAEA_{30}$ polyplexes (Fig. 8c and 8e). The explanation of the polyplex precipitation is that DNA can easily access the charges surrounding the small and soft PnBA core facilitating their effective neutralization and decrease of their solubility.

The ζ-potential values of particles, determined by ELS measurements, are negative at all N/P ratios (Fig. 8b) due to the DNA molecules localization in the periphery of block copolymer micellar aggregates. The polyplexes exhibit negative ζ-potential of higher absolute values at low N/P ratios compared to high N/P ratios due to the presence of a larger number of phosphate groups. The results in Fig. 8a and 8b are in agreement with the complexation behaviour of the $PnBA_{40}$-b-$PDMAEA_{60}$ diblock with nucleic acids as the partially positively charged amino groups of the PDMAEA block have not undergone any chemical modification. Thus, some PDMAEA chains carry insufficient positive charge to strongly bind with the negative phosphate DNA groups. According to Fig. 8d, the $PnBA_{21}$-b-$Q_1PDMAEA_{79}$ based polyplexes are negatively charged at low N/P ratios (0.25 and 0.5) where more phosphate groups exist in solution and are positively charged at high N/P ratios (1.5, 2 and 4) where positively charged amino groups of the copolymer prevail. The $PnBA_{33}$-b-$Q_6PDMAEA_{30}$ polyplexes in Fig. 8f, follow the same line of thought with the $PnBA_{21}$-b-$Q_1PDMAEA_{79}$ polyplexes, presenting negative ζ-potential values at low N/P ratios (0.25 and 0.5) and positive ones at high N/P ratios (1.5, 2 and 4).

3.8. Behaviour of polyplexes in the presence of salt

The stability of the resulting polyplexes regarding in the body-fluids where a considerable concentration of salt is present and modifies electrostatic interactions is of great importance for their effectiveness as gene carriers. In this direction, DLS measurements on DNA/$PnBA_{40}$-b-$PDMAEA_{60}$, DNA/$PnBA_{21}$-b-$Q_1PDMAEA_{79}$ and DNA/$PnBA_{33}$-b-$Q_6PDMAEA_{30}$ polyplexes were performed in solutions with additional salt (original NaCl concentration during complexation was 0.01 M). The solutions of each polyplex system that exhibited the greater stability over time (for a 2-week period), were further studied under the influence of ionic strength. Specifically, the selected solutions for the DNA/$PnBA_{40}$-b-$PDMAEA_{60}$ polyplex system were those at N/P = 1 and 0.5, for the DNA/$PnBA_{21}$-b-$Q_1PDMAEA_{79}$ at N/P = 2 and 0.5, and for the DNA/$PnBA_{33}$-b-$Q_6PDMAEA_{30}$ at N/P = 0.5 and 0.25. Fig. 9 presents the R_h and scattered intensity values as a function of ionic strength for the DNA/$PnBA_{40}$-b-$PDMAEA_{60}$ polyplex at a) N/P = 1 and b) N/P = 0.5 ratios (in deficiency of copolymer). As observed at both N/P ratios, R_h of polyplexes increases with the addition of NaCl, while intensity slightly decreases. The parallel increase in size and decrease in mass leads to the conclusion that addition of salt leads to partial polyplex dissociation due to charge screening effects.

A similar trend occurred for the DNA/$PnBA_{21}$-b-$Q_1PDMAEA_{79}$ polyplexes at both N/P ratios of 2 and 0.5 (in deficiency of polymer), as highlighted in Fig. 10a and 10b. Particularly, the R_h of the polyplexes is increased followed by a decrease in their mass in the presence of salt. As R_h increases, the charged groups of the copolymer and DNA that were initially complexed are now freed, due to the presence of the low molecular weight salt, and thus hydrophilicity of the system is enhanced, leading to a higher incorporation of water molecules and a swelling of the polyplexes. The parallel decline in intensity suggests a decrease in the mass of the polyplexes, indicating their partial disintegration. It is however important that polyplexes exist even at the higher ionic strength utilized. This is indicated by the higher scattering intensity of polyplexes solutions compared to the scattering intensity determined for pure copolymer solutions of similar concentration before complexation.

As seen in Fig. 11a and 11b, the trend of the DNA/$PnBA_{33}$-b-$Q_6PDMAEA_{30}$ polyplex system at both N/P ratios of 0.5 and 0.25, is similar to the previous ones. Lower mass polyplexes with increased diameters are formed upon the addition of salt. By increasing the ionic strength of the solution, the affinity between DNA chains and block copolymers decreases, leading to weaker electrostatic interactions and resulting in partial dissociation of the initially formed polyplexes.

4. Conclusions

The $PnBA_{40}$-b-$PDMAEA_{60}$ diblock copolymer synthesized by RAFT polymerization was successfully converted into $PnBA_{21}$-b-$Q_1PDMAEA_{79}$ and $PnBA_{33}$-b-$Q_6PDMAEA_{30}$ strong cationic, amphiphilic, block polyelectrolytes by quaternization of the tertiary amines of the PDMAEA block using CH_3I and $C_6H_{13}I$ quaternizing agents. DLS results revealed that $PnBA_{21}$-b-$Q_1PDMAEA_{79}$ copolymer chains self-assemble into small micelles of R_h = 20 nm in aqueous solutions, whereas the $PnBA_{33}$-b-$Q_6PDMAEA_{30}$ copolymer forms less well-defined aggregates due to the presence of the six carbons hydrophobic alkyl side chain on the PDMAEA block of the copolymer, inducing hydrophobic interactions between corona chains. The partially positively charged $PnBA_{40}$-b-$PDMAEA_{60}$ diblock and the chemically converted $PnBA_{21}$-b-$Q_1PDMAEA_{79}$ and $PnBA_{33}$-b-$Q_6PDMAEA_{30}$ cationic copolymers, with the latter having a more hydrophobic character, were evaluated for their potential to bind with DNA molecules. FS and UV–Vis

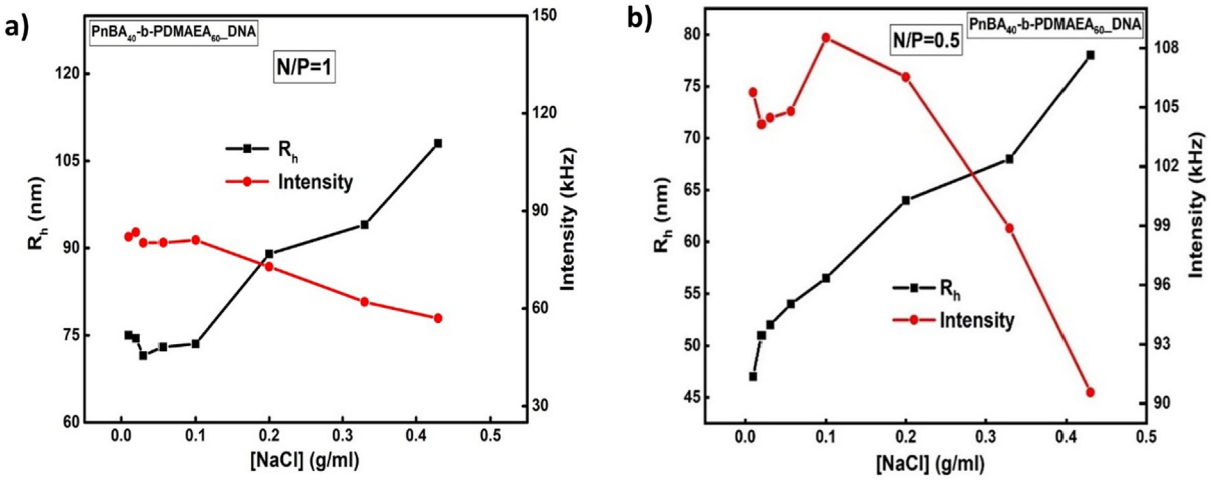

Fig. 9. R_h and scattered intensity as a function of ionic strength ([NaCl]) for DNA/$PnBA_{40}$-b-$PDMAEA_{60}$ polyplexes at (a) N/P = 1 and (b) N/P = 0.5.

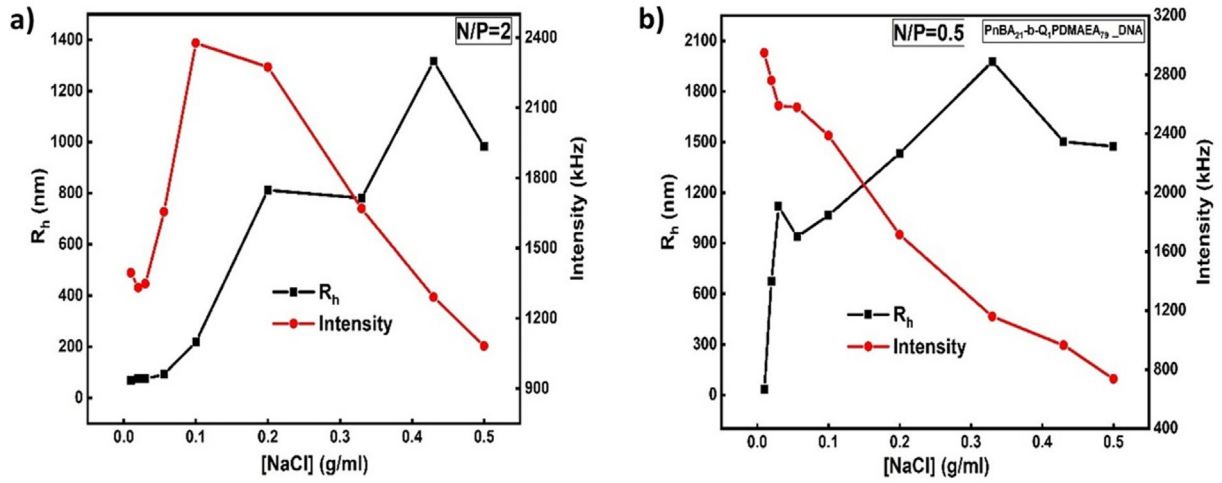

Fig. 10. R_h and scattered intensity as a function of ionic strength ([NaCl]) for DNA/$PnBA_{21}$-b-$Q_1PDMAEA_{79}$ polyplexes at (a) N/P = 2 and (b) N/P = 0.5 ratios.

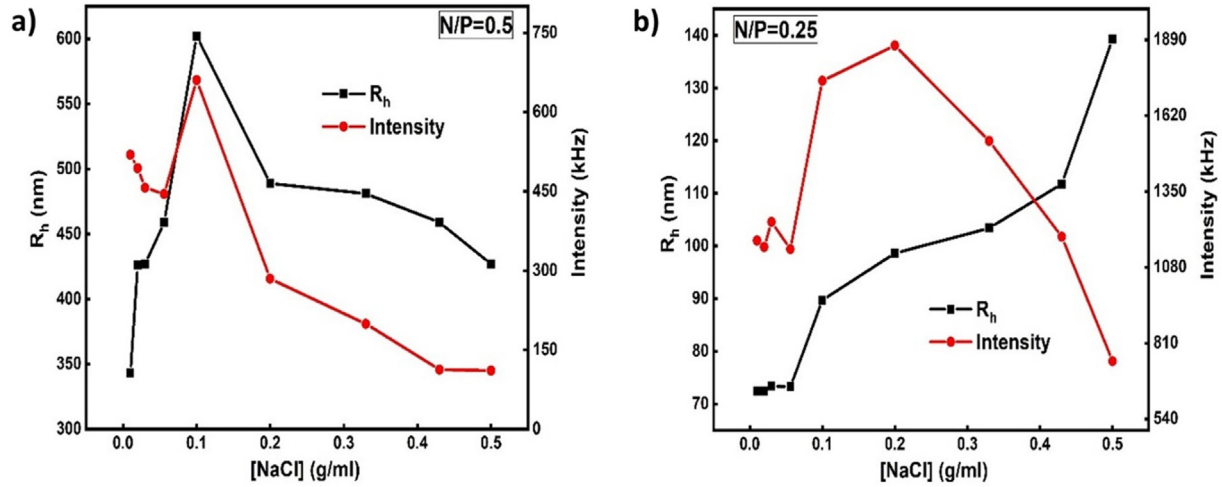

Fig. 11. R_h and scattered intensity as a function of ionic strength ([NaCl]) for DNA/$PnBA_{33}$-b-$Q_6PDMAEA_{30}$ polyplexes at (a) N/P = 0.5 and (b) N/P = 0.25 ratios.

spectroscopies showed a strong binding between cationic $PnBA_{33}$-b-$Q_6PDMAEA_{30}$ quaternized copolymer, with the higher hydrophobic character, and DNA. The low positively charged $PnBA_{40}$-b-$PDMAEA_{60}$ diblock and $PnBA_{21}$-b-$Q_1PDMAEA_{79}$ cationic copolymer were less effective in displacing EtBr and complexation with DNA seems less efficient. Mass, size, surface potential and the ability of the copolymers to interact with DNA molecules revealed a strong dependence on the N/P ratios, as indicated by DLS and ELS techniques, in parallel with the effects of charge density and hydrophobicity of the complexing block. The chemically modified $PnBA_{21}$-b-$Q_1PDMAEA_{79}$ and $PnBA_{33}$-b-$Q_6PDMAEA_{30}$ cationic copolymers showed a strong binding with DNA at almost all N/P ratios without signs of free DNA remaining in the solutions at high N/P ratios. The reinforcing hydrophobic interactions between $Q_6PDMAEA$ chains and DNA in addition to the electrostatic interactions coexisted in the DNA/ polyplex system contributed to the preferential binding, shrinking and compacting of DNA. The physicochemical results of the PDMAEA-based polyplexes give new insights in the parameters affecting block polyelectrolyte/DNA interactions, while the $PnBA_{33}$-b-$Q_6PDMAEA_{30}$ copolymer shows potential as non-viral delivery vector in the field of gene therapy.

Data availability

Data will be available upon request.

Declaration of Competing Interest

The authors declared that there is no conflict of interest.

Appendix A. Supplementary material

Supplementary data to this article can be found online at https://doi.org/10.1016/j.eurpolymj.2020.109636.

References

[1] H. Wang, S. Ding, Z. Zhang, L. Wang, Y. You, Cationic micelle: a promising nanocarrier for gene delivery with high transfection efficiency, J. Gene Med. 21 (2019) e3101, , https://doi.org/10.1002/jgm.3101.
[2] Z. Ge, S. Liu, Functional block copolymer assemblies responsive to tumor and intracellular microenvironments for site-specific drug delivery and enhanced imaging performance, Chem. Soc. Rev. 42 (2013) 7289–7325, https://doi.org/10.1039/c3cs60048c.
[3] A. Kowalczuk, R. Trzcinska, B. Trzebicka, A.H. Mueller, A. Dworak, C.B. Tsvetanov, Loading of polymer nanocarriers: factors, mechanisms and applications, Prog. Polym. Sci. 39 (2014) 43–86, https://doi.org/10.1016/j.progpolymsci.2013.10.004.
[4] M. Imran, M.R. Shah, Shafiullah, Amphiphilic block copolymers–based micelles for drug delivery, in: A.M. Grumezescu (Ed.), Design and Development of New Nanocarriers, William Andrew Publishing, 2018, pp. 365–400.
[5] K. Kataoka, A. Harada, Y. Nagasaki, Block copolymer micelles for drug delivery: design, characterization and biological significance, Adv. Drug Deliver. Rev. 64 (2012) 37–48, https://doi.org/10.1016/j.addr.2012.09.013.
[6] S. Agarwal, Y. Zhang, S. Maji, A. Greiner, PDMAEMA based gene delivery materials,

Mater. Today 15 (2012) 388–393, https://doi.org/10.1016/S1369-7021(12)70165-7.
[7] R. Sharma, J.S. Lee, R.C. Bettencourt, C. Xiao, S.F. Konieczny, Y.Y. Won, Effects of the incorporation of a hydrophobic middle block into a PEG-polycation diblock copolymer on the physicochemical and cell interaction properties of the polymer-DNA complexes, Biomacromolecules 9 (2008) 3294–3307, https://doi.org/10.1021/bm800876v.
[8] N.P. Truong, Z. Jia, M. Burgess, L. Payne, N.A. McMillan, M.J. Monteiro, Self-catalyzed degradable cationic polymer for release of DNA, Biomacromolecules 12 (2011) 3540–3548, https://doi.org/10.1021/bm2007423.
[9] C.M. Wiethoff, C.R. Middaugh, Barriers to nonviral gene delivery, J. Pharm. Sci. 92 (2003) 203–217, https://doi.org/10.1002/jps.10286.
[10] D. Putnam, Polymers for gene delivery across length scales, Nat. Mater. 5 (2006) 439–451, https://doi.org/10.1038/nmat1645.
[11] K.W. Leong, Polymeric controlled nucleic acid delivery, MRS Bull. 30 (2005) 640–646, https://doi.org/10.1557/mrs2005.190.
[12] P. Barthélémy, M. Camplo, Functional amphiphiles for gene delivery, MRS Bull. 30 (2005) 647–653, https://doi.org/10.1557/mrs2005.191.
[13] M. Ahmed, R. Narain, Progress of RAFT based polymers in gene delivery, Prog. Polym. Sci. 38 (2013) 767–790, https://doi.org/10.1016/j.progpolymsci.2012.09.008.
[14] A. Chroni, S. Pispas, A. Forys, B. Trzebicka, pH-driven morphological diversity in poly [n-Butyl acrylate-block-(2-(Dimethylamino) ethyl acrylate)] amphiphilic copolymer solutions, Macromol. Rapid Commun. (2019), https://doi.org/10.1002/marc.201900477.
[15] N.P. Truong, Z. Jia, M. Burges, N.A. McMillan, M.J. Monteiro, Self-catalyzed degradation of linear cationic poly (2-dimethylaminoethyl acrylate) in water, Biomacromolecules 12 (2011) 1876–1882, https://doi.org/10.1021/bm200219e.
[16] T. Manouras, E. Koufakis, S.H. Anastasiadis, M. Vamvakaki, A facile route towards PDMAEMA homopolymer amphiphiles, Soft Matter 13 (2017) 3777–3782, https://doi.org/10.1039/c7sm00365j.
[17] E. Haladjova, G. Mountrichas, S. Pispas, S. Rangelov, Poly(vinyl benzyl trimethylammonium chloride) Homo and Block Copolymers Complexation with DNA, J. Phys. Chem. B 120 (2016) 2586–2595, https://doi.org/10.1021/acs.jpcb.5b12477.
[18] E. Cabane, X. Zhang, K. Langowska, C.G. Palivan, W. Meier, Stimuli-responsive polymers and their applications in nanomedicine, Biointerphases 7 (2012) 9, https://doi.org/10.1007/s13758-011-0009-3.
[19] J.-F. Gohy, Block Copolymer Micelles, in: V. Abetz (Ed.), Block Copolymers II, Springer, Berlin Heidelberg, Berlin, Heidelberg, 2005, pp. 65–136.
[20] A.J. Geall, I.S. Blagbrough, Rapid and sensitive ethidium bromide fluorescencequenching assay of polyamine conjugate–DNA interactions for the analysis of lipoplex formation in gene therapy, Pharm. Biomed. Anal. 22 (2000) 839–859, https://doi.org/10.1016/S0731-7085(00)00250-8.
[21] D. Dey, S. Kumar, R. Banerjee, S. Maiti, D. Dhara, Polyplex formation between PEGylated linear cationic block copolymers and DNA: equilibrium and kinetic studies, J. Phys. Chem. B 118 (2014) 7012–7025, https://doi.org/10.1021/jp501234p.
[22] Y.-W. Kwon, D.H. Choi, J.-I. Jin, Optical, electro-optic and optoelectronic properties of natural and chemically modified DNAs, Polym. J. 44 (2012) 1191–1208, https://doi.org/10.1038/pj.2012.165.